Various Shaped Semiconductor Microlens Arrays Fabricated by Selective Oxidation of AlGaAs

Article *in* IEEE Photonics Technology Letters · November 2009

DOI: 10.1109/LPT.2009.2028083 · Source: IEEE Xplore

5 authors, including:

Ki Soo Chang
Korea Basic Science Institute KBSI
100 PUBLICATIONS **356** CITATIONS
SEE PROFILE

Young Min Song
Gwangju Institute of Science and Technology
217 PUBLICATIONS **4,463** CITATIONS
SEE PROFILE

Geon Hee Kim
Korea Basic Science Institute KBSI
63 PUBLICATIONS **295** CITATIONS
SEE PROFILE

Various Shaped Semiconductor Microlens Arrays Fabricated by Selective Oxidation of AlGaAs

Ki Soo Chang, *Member, IEEE*, Sun Cheol Yang, Young Min Song, Yong Tak Lee, and Geon Hee Kim

***Abstract*—Semiconductor microlens arrays with circular, cylindrical, square, and ring-type bases were fabricated by using selective oxidation of chirped short-period superlattice of GaAs–AlGaAs. Confocal microscopy and atomic force microscopy were used to evaluate the surface morphology of the fabricated microlenses, which revealed that they have cross-sectional profiles close to spherical in shape and an root-mean-square surface roughness of less than 10 nm for the scanned area of 5 μm $\times$ 5 μm. The optical parameters of the microlenses, evaluated by measuring the focused spot pattern and focal length, revealed strong focusing function of the microlenses that were very close to the calculated values, indicating high structural and optical quality of the fabricated microlenses.**

***Index Terms*—AlGaAs, microlens, oxidation, superlattice.**

I. Introduction

DUE TO the ability to manipulate light in a miniature scale, microlens and their arrays have been the key optical components in numerous applications, such as optical communication, free-space optical interconnection, digital imaging, laser beam shaping, solid-state lighting, optical data storage, and laser printers and scanners [1]. In recent years, the insatiable demand for higher optical efficiency and newly emerging applications for microoptical systems and devices have driven the need for various shaped microlenses, not only in circular form, but also in other forms, including cylindrical, square, and ring-type microlenses. Cylindrical microlenses, for example, are very useful in focusing light onto a line and circularizing the astigmatic laser diode output beam. They are used in optical information processing, bar code scanning, and microfluidic sensors [2]–[4]. The fill factor of microlens array, which is defined as the percentage of lens area to the total area, is one of the most important performance criteria of microlens array, especially in IR focal plane arrays (IRFPA), light homogenizers, and laser beam steering applications [5]–[7]. For these applications, square microlens array is preferred to circular microlens array because the microlens array with a square base has a greater fill factor than those with a circular base, which has a maximum fill factor of 78% in an orthogonal arrangement.

Manuscript received May 27, 2009; revised July 09, 2009. First published July 28, 2009; current version published September 18, 2009. This work was supported by Korea Basic Science Institute under Grant N28081 and Grant D29200.

K. S. Chang, S. C. Yang, and G. H. Kim with the Division of Instrument Development, Korea Basic Science Institute, Daejeon 305-333, Korea (e-mail: ksc@kbsi.re.kr; md941057@kbsi.re.kr; kgh@kbsi.re.kr).

Y. M. Song and Y. T. Lee are with the Department of Information and Communications, Gwangju Institute of Science and Technology, Gwangju 500-712, Korea (e-mail: ymsong@gist.ac.kr; ytlee@gist.ac.kr).

Digital Object Identifier 10.1109/LPT.2009.2028083

GaAs cap (100 nm)
$Al_{0.98}Ga_{0.02}As$ (90 ML)
GaAs (4ML)
$Al_{0.98}Ga_{0.02}As$ (89 ML)
GaAs (4ML)
⋮
$Al_{0.98}Ga_{0.02}As$ (17 ML)
GaAs (4ML)
$Al_{0.98}Ga_{0.02}As$ (16 ML)
GaAs buffer (100 nm)
GaAs substrate

Fig. 1. Schematic diagram of the composition-graded Al_x $Ga_{1-x}As$ $(x = 0.8–0.96)$, utilizing chirped short-period superlattice of $Al_{0.98}Ga_{0.02}As$ (16–90 monolayers)–GaAs (four monolayers).

In addition, ring-shaped microoptical structures, applicable to photonic quantum ring lasers, microring resonators, and LEDs in a ring format, have recently attracted much attention [8]–[10]. Fabrication of microlens arrays in AlGaAs alloy system enables monolithic, as well as hybrid, integration of these microlens arrays on or in the optoelectronic devices with AlGaAs–GaAs heterostructures, such as LEDs, laser diodes, photodetectors, IR image sensors, and waveguides. Recently, we observed that the convex-lens-shaped oxidation profiles can be formed by selective oxidation of composition-graded AlGaAs due to the strong dependence of the oxidation rate on Al composition of AlGaAs [11].

In this letter, we extend the application of the selective oxidation of composition-graded AlGaAs technique to the fabrication of refractive microlens arrays in any kind of form. Manifold-shaped microlens arrays, including not only circular, but also cylindrical, square, and ring-type microlenses, could be fabricated by simply changing photomask patterns. We also present the optical performance of the fabricated microlens arrays.

II. Growth and Fabrication

By properly designing the epitaxial layer structure and photomask pattern, manifold-shaped microlens arrays could be fabricated using a selective oxidation method. Fig. 1 shows an epitaxial layer structure of the composition-graded AlGaAs, utilizing chirped short-period superlattice of $Al_{0.98}Ga_{0.02}As$–GaAs. The epitaxial layer structure was grown by solid source molecular beam epitaxy (SSMBE) system. A 1.3-μm-thick AlGaAs layer, in which the average Al composition is linearly graded from 0.8 to 0.96 along the growth direction, was grown on the GaAs buffer layer. The chirped short-period superlattice of $Al_{0.98}Ga_{0.02}As$ (16–90 monolayers)–GaAs (four monolayers) was used to grade the composition of AlGaAs. The thickness of GaAs layer was fixed

by four monolayers, while the thickness of $Al_{0.98}Ga_{0.02}As$ layer varied from 16 to 90 monolayers along the growth direction. The structure was then capped with a 100-nm-thick GaAs cap layer, which prevents oxidation from the top surface of AlGaAs layer. This chirped short-period superlattice technique, also termed digital-alloy technique, provided a versatile, accurate, and reproducible control of the composition compared to the analog alloy. In addition, a thin GaAs layer in short-period superlattice acted as a vertical oxidation barrier, resulting in a convex-lens-shaped oxidation front after selective oxidation with a simple linear composition grading of AlGaAs [11].

After the growing process, microlens fabrication processes started with a definition of circular, stripe, square, and ring-shaped mesas by standard photolithography and inductively coupled plasma (ICP) dry etching to expose the composition-graded AlGaAs layer at the mesa sidewall for lateral oxidation. A wet thermal oxidation process was carried out at a temperature of 410 °C for 80 min in a tube furnace with water vapor, which was supplied using nitrogen, bubbling through a water bath kept at 94 °C. The flow rate of the nitrogen carrier gas was 2 L/min. After oxidation, the GaAs cap layer was selectively etched by 10 : 1 citric acid : H_2O_2 solution, and then, the Al oxide covering the AlGaAs microlens was selectively removed in 1 : 5 KOH (45% with water) : H_2O solution, leaving only the AlGaAs microlenses.

From this technique, circular, cylindrical, and square microlens arrays with nominal array pitch and spacing of 30 and 2 μm, respectively, and ring-shaped microlenses with a nominal inner diameter and base width of 100 and 30 μm, respectively, were fabricated. The fabricated microlens arrays were characterized without any protective or antireflective coatings.

III. Structural and Optical Characterization

To evaluate the surface morphology of the fabricated microlenses, 3-D surface profiles were measured by confocal microscopy (NanoFocus, μSurf). The cross-sectional profiles along the line passing through the center of the microlenses were also extracted from topological images, as shown in Fig. 2. It can be seen that the manifold-shaped plano-convex microlenses are well defined and the overall cross-sectional profiles closely fit with the circles. The base width (or diameter) and height of the microlenses were measured to be 25.6–25.8 μm and 1.23–1.26 μm, respectively, which were slightly different for each lens shape. The radius of curvature (ROC) estimated from circular fit ranged between 70.6 and 74.4 μm. Square microlenses were "arch dome" in shape, as shown in Fig. 2(c), while circular microlenses had near spherical surfaces. The ROC of square microlens varied from a minimum of 74.4 μm along the horizontal axis of the sides to a maximum of 141.6 μm along the diagonal axis of the square.

To determine the roughness of the microlens surface, we measured an atomic force microscopy (AFM) surface profile of a randomly selected portion of the microlens surface, as shown in Fig. 3. The root-mean-square (rms) roughness values of all microlenses were less than 10 nm for the scanned area of 5 μm $\times$ 5 μm, thus ensuring a high surface quality of microlenses. The measured structural characteristics of the fabricated microlens arrays are summarized in Table I.

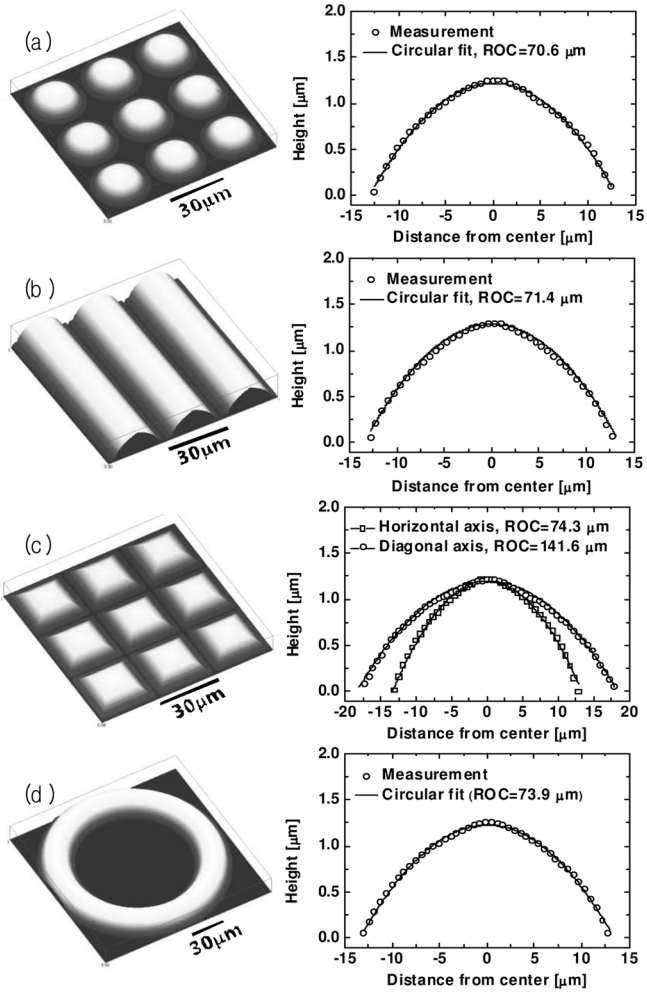

Fig. 2. (Left column) 3-D surface profiles of the fabricated microlens arrays measured by confocal microscopy. (Right column) Cross-sectional profiles along the line passing through the center of the microlenses. (a) Circular microlens array, pitch: 30 μm. (b) Cylindrical microlens array, pitch: 30 μm. (c) Square microlens array, pitch: 30 μm. (d) Microring lens, ring width: 30 μm and inner diameter: 100 μm.

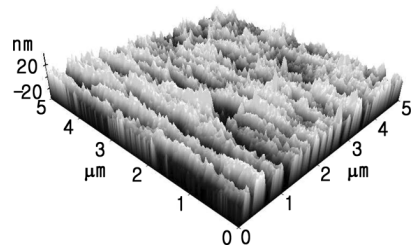

Fig. 3. Surface topography imaged by an AFM in a randomly selected area of 5 μm $\times$ 5 μm on a cylindrical microlens. The measured rms surface roughness is 8.2 nm.

In order to analyze the optical characteristics of the fabricated microlens arrays, the focal length and the 2-D beam spot pattern were measured. Fig. 4 shows the intensity distribution of the laser beam at the focal plane of the microlens arrays. The sharp focused light spots, lines, and ring are clearly observed for circular, cylindrical, and ring-shaped microlens arrays, respectively. The measured spot sizes with a full width of $1/e^2$ intensity of the peak for circular, cylindrical, and ring-shaped

TABLE I
STRUCTURAL AND OPTICAL CHARACTERISTICS OF THE FABRICATED MICROLENSES

Parameters	Base shape			
	Circular	Cylindrical	Square	Ring
Base width (or dia.) [μm]	25.6	25.6	25.7	25.8
Height [μm]	1.24	1.26	1.23	1.26
ROC (fit) [μm]	70.6	71.4	74.4 (H*) 141.6 (D*)	73.9
Surface roughness (RMS) [nm]	9.4	8.2	9.1	9.8
Focal length [μm]	36±1	38±1	-	38±1
Spot width (or dia.) [μm]	5.1	5.1	-	5.2

* H: Horizontal axis, D: Diagonal axis

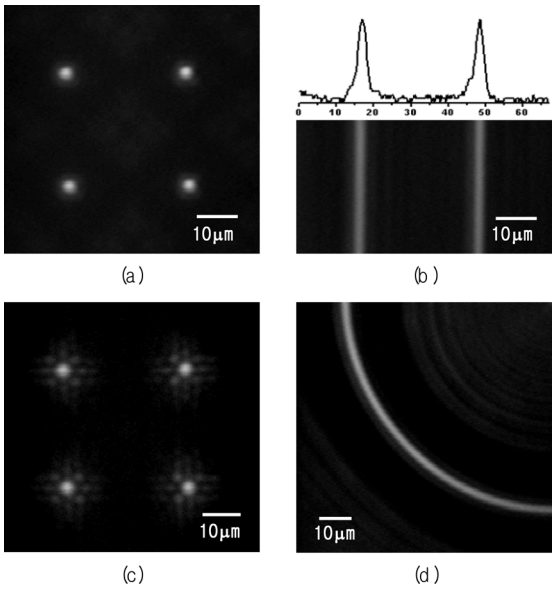

Fig. 4. Laser beam intensity distribution on the focal plane of the microlens arrays with: (a) circular, (b) cylindrical, (c) square, and (d) ring-type bases. [Inset top in (b)] Laser beam intensity profile. Laser wavelength is 1550 nm.

microlenses were 5.1, 5.1, and 5.2 μm, respectively. The intensity profiles were quite uniform, not only along the lens, but also from lens to lens, and the pitch of the focused light spot was also uniform and the same as the designed value of 30 μm. Fig. 4(c) shows laser beam intensity distribution measured on the quasi-confocal plane of square microlens array, 45 μm apart from the microlens surface. The parasitic spots around the bright spot at the center of microlens can be attributed to the interference pattern caused by different focal lengths of 37.8 and 71.9 μm for the diagonal and horizontal axes of the square microlens, respectively. These focal length difference and parasitic spots make it difficult to define the exact focal length and spot diameter for the square microlens array. Although the square microlens array produced spots less sharp than the spots focused by the circular microlens array, they are quite useful to IRFPA application because they can effectively concentrate light onto the active areas of a detector array, and provide a larger fill factor than that of the orthogonal array of circular microlenses. The focal length of the circular, cylindrical, and ring-shaped microlenses was measured as 36 ± 1, 38 ± 1, and 38 ± 1 μm, respectively, which are very close to the calculated values of 35.8, 36.2, and 37.5 μm, respectively, with an average refractive index of 2.97 for $Al_xGa_{1-x}As$ $(x = 0.8\text{–}0.96)$ and an estimated ROC from the circular fit. These results indicate that the microlens arrays fabricated by the selective oxidation method have high structural and optical consistency.

IV. CONCLUSION

We fabricated various shaped semiconductor microlens arrays, including those with circular, cylindrical, square, and ring-type bases, by using selective oxidation of chirped short-period superlattice of GaAs–AlGaAs. The structural and optical characterization tests demonstrate that the fabricated microlens arrays have good surface quality and optical properties. This microlens fabrication method is versatile in making a wide range of semiconductor microlens arrays in terms of size, fill factor, and shape, which offer a variety of applications, especially when integrated with semiconductor photonic devices to required light manipulation.

REFERENCES

[1] S. Sinzinger and J. Jahns, *Microoptics*. New York: Wiley/VCH, 2003.
[2] J. J. Snyder, "Cylindrical micro-optics," in *Proc. SPIE*, 1993, vol. 1992, pp. 235–246.
[3] Y. Fu, N. K. A. Bryan, and O. N. Shing, "Integrated micro-cylindrical lens with laser diode for single-mode fiber coupling," *IEEE Photon. Technol. Lett.*, vol. 12, no. 9, pp. 1213–1215, Sep. 2000.
[4] S. Huang and F. Tseng, "Development of a monolithic total internal reflection-based biochip utilizing a microprism array for fluorescence sensing," *J. Micromech. Microeng.*, vol. 15, pp. 2235–2242, 2005.
[5] M. He, X. Yuan, K. J. Moh, J. Bu, and X. Yi, "Monolithically integrated refractive microlens array to improve imaging quality of an infrared focal plane array," *Opt. Eng.*, vol. 43, no. 11, pp. 2589–2594, 2004.
[6] J. Pan, C. Wang, H. Lan, W. Sun, and J. Chang, "Homogenized LED-illumination using microlens arrays for a pocket-sized projector," *Opt. Express*, vol. 15, no. 17, pp. 10483–10491, 2007.
[7] A. Akatay, C. Ataman, and H. Urey, "High-resolution beam steering using microlens arrays," *Opt. Lett.*, vol. 31, no. 19, pp. 2861–2863, 2006.
[8] O. D. Kwon, J. H. Yoon, D. K. Kim, Y. C. Kim, S. E. Lee, and S. S. Kim, "Mega-pixel PQR laser chips for interconnect, display ITS, and biocell-tweezers OEIC," in *Proc. SPIE*, 2008, vol. 6897, pp. 68970V-1–68970V-10.
[9] V. Van, T. A. Ibrahim, K. Ritter, P. P. Absil, F. G. Johnson, R. Grover, J. Goldhar, and P.-T. Ho, "All-optical nonlinear switching in GaAs-AlGaAs microring resonators," *IEEE Photon. Technol. Lett.*, vol. 14, no. 1, pp. 74–76, Jan. 2002.
[10] H. W. Choi, M. D. Dawson, P. R. Edwards, and R. W. Martin, "High extraction efficiency InGaN micro-ring light-emitting diodes," *Appl. Phys. Lett.*, vol. 83, no. 22, pp. 4483–4485, 2003.
[11] K. S. Chang, Y. M. Song, and Y. T. Lee, "Microlens fabrication by selective oxidation of composition-graded digital alloy AlGaAs," *IEEE Photon. Technol. Lett.*, vol. 18, no. 1, pp. 121–123, Jan. 2006.